Correlation Between Conducted Injection and Near-Field Scan Immunity in the L-Band

Nicolas Castagnet, Alexandre Boyer, Fabien Escudié

Correlation Between Conducted Injection and Near-Field Scan Immunity in the L-Band

Nicolas Castagnet
CEA, DAM, CEA-Gramat
F-46500 Gramat, France
LAAS-CNRS
Toulouse, France
nicolas.castagnet@cea.fr

Alexandre Boyer
LAAS-CNRS, INSA Toulouse
Toulouse, France
alexandre.boyer@laas.fr

Fabien Escudié
CEA, DAM, CEA-Gramat
F-46500 Gramat, France
fabien.escudie@cea.fr

***Abstract*—Near-Field Scan Immunity (NFSI) is a recent method for analyzing the electromagnetic (EM) susceptibility of an integrated circuit (IC), allowing the study of a system behavior subject to an intentional electromagnetic interference (IEMI). It is a non-intrusive technique that can precisely target component pins that are otherwise inaccessible. This paper compares NFSI to a conducted injection method inspired by the direct power injection (DPI) standard and presents a correlation between the two injection techniques between 500 MHz and 2 GHz. The numerical and experimental validation with different types of near-field probes is validated on passive linear loads.**

***Keywords*—electromagnetic compatibility (EMC), intentional electromagnetic interference (IEMI), near-field scan immunity (NFSI), direct power injection (DPI)**

I. Introduction

In electronic systems, sophisticated and compact electronic components are increasingly used and potentially more vulnerable to failure in case of an IEMI. Vulnerability measurement of such systems is typically conducted during radiated immunity tests [1], [2], and the DPI method is employed to precisely analyze the behavior of ICs [3]. However, it is highly intrusive, requiring the presence of a radiofrequency (RF) connector mounted on the tested board, and it does not take into account the real electromagnetic environment in which the component operates. In addition, the output impedance of the RF generator can influence the operation of the device under test (DUT).

Near-field scan immunity (NFSI), as detailed by its IEC technical specification [4] also provides a precise injection of RF disturbances focusing on a component pin or a circuit board trace, while allowing the entire system to operate under nominal conditions. This method enables the identification of failures without changing the design of the system [5], [6] but, as the aggression is injected into the DUT without direct contact, the coupling of the disturbance is different from that appearing in the case of a conducted injection. Therefore, the link between failure thresholds measured in conducted injection and NFSI is not straightforward and has no precedent in the literature. In this paper, a methodology for estimating conducted voltage on the DUT based on the voltage injected in the near-field injection set-up is proposed. The aim is to validate the method in simple cases and for a frequency range between 500 MHz and 2 GHz.

This study has been carried out with the support of the French Ministry of Defense - Defense Innovation Agency.

In the first part, a transfer function is established for each technique (NFSI and DPI) using their S-parameters. The experimental validation of the model is then conducted with two types of near-field injection probes on several loads with different impedances (real and complex).

II. Modeling of electromagnetic susceptibility measurement methods

A. Equivalent Model of the Direct Power Injection (DPI)

The aim of the DPI is to apply an RF disturbance to a pin of an IC to quantify the amplitude required for the occurrence of a failure (usually measured as the forward power captured through a bidirectional coupler and an RF power meter). As shown in Fig. 1, the harmonic disturbance is produced by an RF signal generator and then injected into the DUT through a bidirectional coupler and a high-pass filter (bias tee) that blocks the DC voltage.

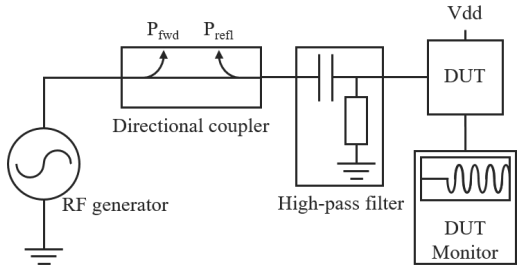

Fig. 1. Direct power injection (DPI) measurement set-up.

Modeling the DPI set-up involves characterizing the key elements of the schematic. The equivalent model of the DPI test is described in Fig. 2. The DUT is represented by its impedance Z_{DUT} connected to the aggression path, itself modeled by transmission lines representing the cables as

well as the transfer functions of the set-up elements such as the directional coupler. S_{21}^{DPI} is defined as the transmission coefficient between ports P1 (RF generator output) and P2 (measurement point of the voltage applied to the component).

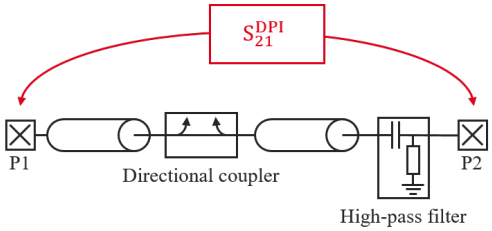

Fig. 2. Equivalent model of the DPI method.

This definition of the equivalent model for DPI is the foundation for the following comparison with the NFSI method.

B. Near-Field Injection Model

The NFSI technique is based on the use of a miniature probe (with diameters ranging from hundreds of micrometers to millimeters) generating a magnetic H-field or an electric E-field near the DUT. The coupling of this field onto the DUT induces voltage fluctuations across the pins of the IC that may lead to component failure. The aggression path of NFSI is described in Fig. 3. As before, S_{21}^{NFSI} is the near-field transmission coefficient. This transfer function depends on the coupling between the probe and the IC, involving parameters such as frequency, trace characteristics, and also the location and geometry of the injection probe. A preliminary calibration phase is needed to ensure results reproducibility [7], [8] and to determine the voltage or current induced on line termination by the injection probes.

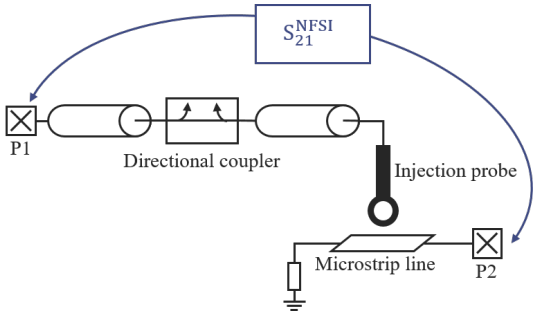

Fig. 3. Equivalent model of the Near-Field Scan Immunity (NFSI) test.

C. Establishing Theoretical Equivalence

It is assumed that a failure occurs at the DUT at a given frequency for an amplitude V_{DUT} applied to one pin of the component, represented by its impedance Z_{DUT}, constant whatever the injection set-up used and the frequency. Fig. 4 shows the equivalent schematic of the models presented in the previous section as an S-parameter box. V_G and Z_G are respectively the equivalent amplitude and impedance of the RF generator.

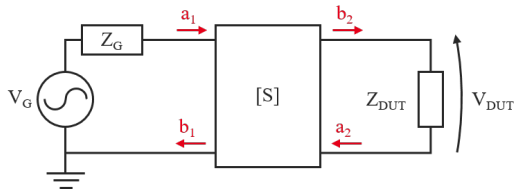

Fig. 4. Diagram of the aggression path with an S-parameters box.

1) General equations: Let Z_C be the real characteristic impedance of the line. The reflection coefficients of the load Γ_{DUT} and the source Γ_G are defined by (1) and (2).

$$\Gamma_{DUT} = \frac{Z_{DUT} - Z_C}{Z_{DUT} + Z_C} \tag{1}$$

$$\Gamma_G = \frac{Z_G - Z_C}{Z_G + Z_C} \tag{2}$$

Let's define ρ, the reflection coefficient seen from port 1 of the S-parameters box.

$$\rho = S_{11} + \frac{\Gamma_{DUT} S_{12} S_{21}}{1 - \Gamma_{DUT} S_{22}} \tag{3}$$

Knowing that $a_1 = \frac{V_G}{2} \cdot \frac{1-\Gamma_G}{1-\rho\Gamma_G}$, we can write according to (3):

$$a_1 = \frac{V_G}{2} \cdot \frac{(1-\Gamma_G)(1-\Gamma_{DUT}S_{22})}{(1-\Gamma_G S_{11})(1-\Gamma_{DUT}S_{22}) - \Gamma_G\Gamma_{DUT}S_{12}S_{21}} \tag{4}$$

Similarly, we know that $b_2 = S_{21}a_1 + S_{22}a_2$ and $a_2 = \Gamma_{DUT} b_2$ so $b_2 = a_1 S_{21}/(1-\Gamma_{DUT}S_{22})$ and according to (4):

$$b_2 = \frac{V_G}{2} \cdot \frac{S_{21}(1-\Gamma_G)}{(1-\Gamma_G S_{11})(1-\Gamma_{DUT}S_{22}) - \Gamma_G\Gamma_{DUT}S_{12}S_{21}} \tag{5}$$

The voltage V_{DUT} applied across the component's pins is $V_{DUT} = b_2(1+\Gamma_{DUT})$. Combined with (5), the expression of the voltage to the DUT is given by (6).

$$V_{DUT} = \frac{V_G}{2} \cdot \frac{S_{21}(1-\Gamma_G)(1+\Gamma_{DUT})}{(1-\Gamma_G S_{11})(1-\Gamma_{DUT}S_{22}) - \Gamma_G\Gamma_{DUT}S_{12}S_{21}} \tag{6}$$

2) Specific case: An injection set-up should be designed with the most adapted components as possible. In a conducted injection test like the DPI, $Z_G = Z_C$ and $S_{11} = S_{22} = 0$. But this last statement is valid in NFSI only if the microstrip line is 50 Ω adapted. In this case, (6) turns to (7).

$$V_{DUT} = \frac{V_G}{2} \cdot S_{21}(1+\Gamma_{DUT}) \tag{7}$$

If a failure occurs for an amplitude V_{DUT}^{DPI} during a DPI test, it also appears when the same voltage is applied to the component with a near-field probe. Thus, $V_{DUT}^{DPI} = V_{DUT}^{NFSI}$, leading to (8) and (9).

$$\frac{V_G^{DPI}}{2} \cdot S_{21}^{DPI}(1+\Gamma_{DUT}) = \frac{V_G^{NFSI}}{2} \cdot S_{21}^{NFSI}(1+\Gamma_{DUT}) \tag{8}$$

$$V_G^{DPI} S_{21}^{DPI} = V_G^{NFSI} S_{21}^{NFSI} \tag{9}$$

The relationship between the amplitude required in both set-ups for the appearance of the same failure is described in (10).

$$V_G^{NFSI} = V_G^{DPI} \cdot \frac{S_{21}^{DPI}}{S_{21}^{NFSI}} \tag{10}$$

This equation allows the prediction of the conducted immunity level from the NFSI results.

III. Experimental Validation on Linear Loads with Two Types of Injection Probes

A. Calibration of Near-Field Injection Probes

The components (couplers, cables, traces, etc.) used in both aggression chains (DPI and NFSI) are designed to be 50 Ω adapted over the studied frequency range. Their S-parameters are characterized using a Vector Network Analyzer in order to extract the S_{21}^{DPI} and S_{21}^{NFSI} functions. The model has been tested using two injection probes with different types of coupling: a LANGER SX-R 3-1 H-field probe with a diameter of 1 mm, and a LANGER SX-E 03 E-field probe with an emission surface of 4x4 mm. As described in Fig. 5, the 50 Ω adapted microstrip line used for the calibration has been designed on an FR4 substrate terminated by two 50 Ω adapted SMA connectors. It has an effective dielectric parameter $\epsilon_r = 4.5$, a length $L = 40$ mm, a metallization width $w = 3$ mm, a height $h = 1.5$ mm and a copper thickness $T = 35$ µm. Fig. 6 shows the measurement results of the transmission coefficient between each probe and the microstrip line situated 500 µm below.

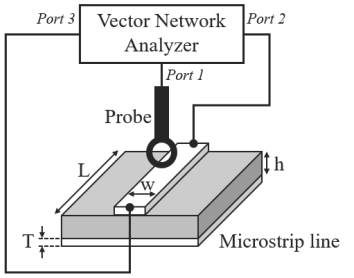

Fig. 5. Calibration set-up of a near-field injection probe.

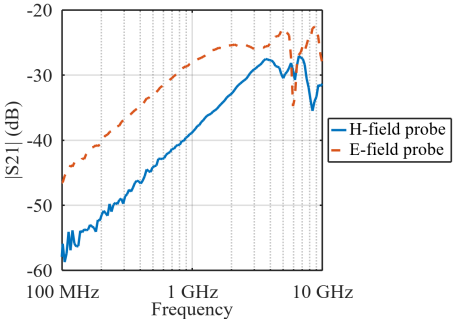

Fig. 6. Measurement of the transmission coefficient between the injection probes and a microstrip line (probe height = 500 µm).

The coupling of the two probes remains almost constant up to 3 GHz. It is very low below 200 MHz so the power supplied by the RF generator must be significant. The use of an RF amplifier may be useful, but its gain depends on the frequency and must be taken into account in the calculation of the system's transfer function, while paying attention to the breakdown voltage and the fusing current of the probe (to avoid damaging it). The resonance at 6 GHz is caused by a reflection of the microstrip line. The functions K_E and K_H are the correction to be applied in the near-field injection method to determine DPI results when using an E-field or an H-field injection probe. These functions are determined from (10).

$$K_E = \frac{S_{21}^{DPI}}{S_{21}^{NFSI}|_E} \tag{11}$$

$$K_H = \frac{S_{21}^{DPI}}{S_{21}^{NFSI}|_H} \tag{12}$$

Fig. 7 shows the measured transfer functions in conducted mode $\left(S_{21}^{DPI}\right)$, in near-field with an H-field probe $\left(S_{21}^{NFSI}|_H\right)$ or with an E-field probe $\left(S_{21}^{NFSI}|_E\right)$, as well as the corrective functions K_E and K_H.

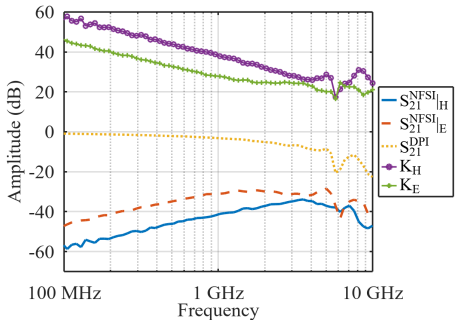

Fig. 7. Transfer functions of the two susceptibility measurement methods (DPI and NFSI) as a function of magnetic or electric coupling, along with K_H and K_E corrective functions.

The decrease of S_{21}^{DPI} is due to power losses in the agression path. The amplitude V_G^{DPI} of the CW signal created by the RF generator during a conducted aggression is maintained constant for the entire frequency range under study. In contrast and as mentioned in (10), the source voltage for NFSI is changed according to the frequency and the type of coupling in order to induce the same level of voltage across the DUT.

B. Experimental Results on Real Impedances

Due to the weak coupling at low frequency of the near-field injection probes and the present limitations of the experimental measurement set-up at high frequencies (the oscilloscope bandwidth is 2.5 GHz), it was decided to work around the L-band, i.e. between 500 MHz and 2 GHz. An initial validation of the correlation between DPI and NFSI for two types of coupling is performed on purely resistances which exhibits a stable impedance over the entire study range. Fig. 8 shows the amplitude in dBV measured at the terminals of 20 Ω and 1 kΩ SMD resistors.

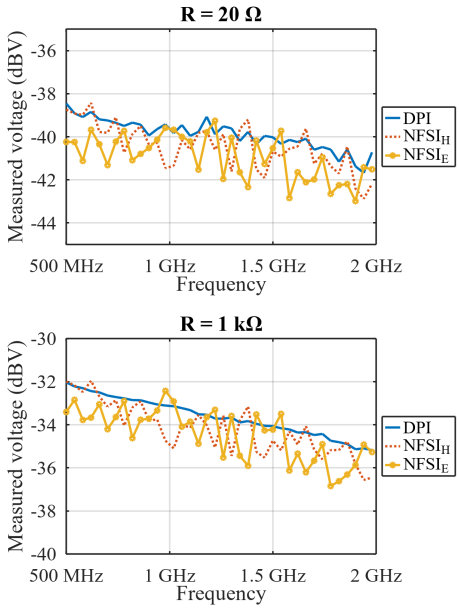

Fig. 8. Comparison of voltages across real loads for different injection techniques (DPI, NFSI with H-field and E-field probes).

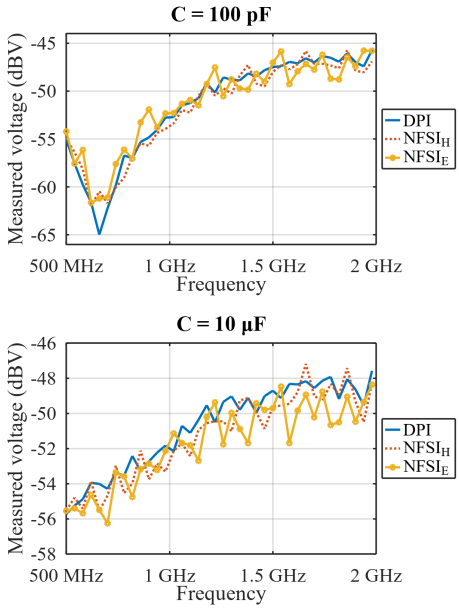

Fig. 9. Comparison of voltages across complex loads for different injection techniques (DPI, NFSI with H-field and E-field probes).

A good agreement is observed for both near-field injection types, which validates the model established in this paper. The small variation between conducted and near-field injection results (average error = 0.6 dB and maximum error = 2 dB) arises from the uncertainty of positionning the probes above the line. The study has been conducted with five other resistance values yielding similar results.

C. Experimental Results on Complex Impedances

The same experiment has been repeated with complex impedance. Fig. 9 shows the amplitude in dBV measured across 100 pF and 10 µF SMD capacitors whose impedances are complex for the DPI and NFSI methods. The resonance frequency of the 100 pF capacitor at 650 MHz explains the frequency response of the first graph in Fig. 9. The average error for these two capacitors is 0.7 dB, and the maximum error is 4 dB because of the resonance.

These two simple case studies validate the near-field and conducted injection correlation model for H-field and E-field coupling on linear passive components.

IV. Conclusion

Near-Field Scan Immunity is a promising technique for analyzing the electromagnetic susceptibility of an integrated circuit in a non-intrusive way. This paper has presented a method to correlate the NFSI technique to a conducted one (DPI), which was validated on linear passive loads for both magnetic and electric coupling. Further works should extend the methodology on more complex components such as non-linear components, ICs and unknown impedance. The equivalence between near-field injection and conducted injection should also be extended to higher frequency bands.

Acknowledgment

This study has been carried out with the support of the French Ministry of Defense - Defense Innovation Agency.

References

[1] V. Houchouas, J. L. Esteves, E. Cottais, C. Kasmi and K. Armstrong, "Immunity assessment of a servomotor exposed to an intentional train of RF pulses," 2017 International Symposium on Electromagnetic Compatibility - EMC Europe, Angers, France, 2017.

[2] R. Sakai, K. Watanabe, S. Ashida, H. Uehara, S. Tanaka and M. Nagata, "Impact of Emission Noise and Electromagnetic Shielding on Mobile Communication Systems in Unmanned Aerial Vehicles," 2023 International Symposium on Electromagnetic Compatibility – EMC Europe, Krakow, Poland, 2023.

[3] IEC 62132-4: Integrated Circuits, Measurement of Electromagnetic Immunity, 150 kHz to 1 GHz - Part 4: Direct RF power injection method, International Electrotechnical Commission, 2014.

[4] IEC TS 62132-9, Integrated circuits – Measurement of electromagnetic immunity – Part 9: Measurement of radiated immunity – Surface scan method, International Electrotechnical Commission, 2014.

[5] A. Boyer, B. Vrignon, and J. Shepherd, "Near-Field Injection at Die Level". In 2015 Asia-Pacific Symposium on Electromagnetic Compatibility (APEMC), 478 81. Taipei: IEEE, 2015.

[6] M. Zouaoui, E. Sicard, H. Braquet, G Rudelou, E. Marsy, and G. Jacquemod, "Impact of NFSI on the Clock Circuit of a Gigabit Ethernet Switch". In 2017 11th International Workshop on the Electromagnetic Compatibility of Integrated Circuits (EMCCompo), 131 35. Saint Petersburg, Russia: IEEE, 2017.

[7] M. Krause and M. Leone, "Calibrated time-domain nearfield-immunity test on printed-circuit board level," 2013 International Symposium on Electromagnetic Compatibility, Brugge, Belgium, 2013, pp. 693–698.

[8] A. Boyer, N. Nolhier, F. Caignet and S. B. Dhia, "On the Correlation Between Near-Field Scan Immunity and Radiated Immunity at Printed Circuit Board Level – Part I," in IEEE Transactions on Electromagnetic Compatibility, vol. 64, no. 4, pp. 1230–1242, Aug. 2022.